Author's Accepted Manuscript

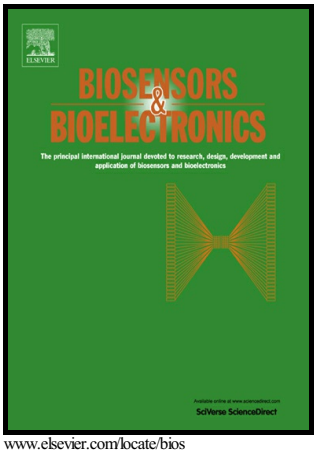

www.elsevier.com/locate/bios

Immunodetection of salivary biomarkers by an optical microfluidic biosensor with polyethylenimine-modified polythiophene-C_{70} organic photodetectors

Tao Dong, Nuno Miguel Matos Pires

PII: S0956-5663(17)30156-2
DOI: http://dx.doi.org/10.1016/j.bios.2017.03.005
Reference: BIOS9593

To appear in: *Biosensors and Bioelectronic*

Received date: 15 January 2017
Revised date: 4 March 2017
Accepted date: 5 March 2017

Cite this article as: Tao Dong and Nuno Miguel Matos Pires, Immunodetectio of salivary biomarkers by an optical microfluidic biosensor wit polyethylenimine-modified polythiophene-C_{70} organic photodetectors *Biosensors and Bioelectronic,* http://dx.doi.org/10.1016/j.bios.2017.03.005

This is a PDF file of an unedited manuscript that has been accepted fo publication. As a service to our customers we are providing this early version o the manuscript. The manuscript will undergo copyediting, typesetting, an review of the resulting galley proof before it is published in its final citable form Please note that during the production process errors may be discovered whic could affect the content, and all legal disclaimers that apply to the journal pertain

ACCEPTED MANUSCRIPT

Immunodetection of salivary biomarkers by an optical microfluidic biosensor with polyethylenimine-modified polythiophene-C_{70} organic photodetectors

Tao Dong[c,*1], Nuno Miguel Matos Pires[a,b,1]

[a]Institute of Applied Micro-Nano Science and Technology, Chongqing Key Laboratory of Micro-Nano Systems Technology and Smart Sensing, Chongqing Technology and Business University, Nan'an District, Chongqing 400067, China
[b]Chongqing Engineering Laboratory for Detection, Control and Integrated System, National Research Base of Intelligent Manufacturing Service, Chongqing Technology and Business University, Nan'an District, Chongqing 400067, China
[c]Institute for Microsystems - IMS, Faculty of Technology, Natural Sciences and Maritime Sciences, University College of Southeast Norway, Postboks 235, 3603 Kongsberg, Norway

[*]Author to whom any correspondence shall be addressed, Tel: +47 31009321, E-mail: tao.dong@usn.no

Abstract.

This work reports a novel optical microfluidic biosensor with highly sensitive organic photodetectors (OPDs) for absorbance-based detection of salivary protein biomarkers at the point of care. The compact and miniaturized biosensor has comprised OPDs made of polythiophene-C_{70} bulk heterojunction for the photoactive layer; whilst a calcium-free cathode interfacial layer, made of linear polyethylenimine, was incorporated to the photodetectors to enhance the low cost. The OPDs realized onto a glass chip were aligned to antibody-functionalized chambers of a poly(methyl methacrylate) microfluidic chip, in where immunogold-silver assays were conducted. The biosensor has detected IL-8, IL-1β and MMP-8 protein in spiked saliva with high detection specificity and short analysis time exhibiting detection limits between 80 pg mL^{-1} and 120 pg mL^{-1}. The result for IL-8 was below the clinical established cut-off of 600 pg mL^{-1}, which revealed the potential of the biosensor to early detection of oral cancer. The detection limit was also comparable to other previously reported immunosensors performed with bulky instrumentation or using industrial inorganic photodetectors. The optical detection sensitivity of the polythiophene-C_{70} OPDs were enhanced by optimizing the thickness of the photoactive layer and anode interfacial layer prior to the saliva immunoassays. Further, the biosensor was tested with unspiked human saliva samples, and the results of measuring IL-8 and IL-1β were in statistical agreement with those provided by two commercial assays of ELISA. The optical microfluidic biosensor reported hereby offers an attractive and cost-effective tool to diagnostics or screening purposes at the point of care.

Keywords:
Immunosensor; saliva diagnostics; optical biosensor; integrated microfluidics; organic photodetector; point-of-care

[1] The authors contributed equally and shared the first authorship

Accepted manuscript

ACCEPTED MANUSCRIPT

1 Introduction

Rapid, highly sensitive, and high-throughput detection of proteins is often a crucial step in clinical diagnostics and patient treatment. Certain diseases, such as cancer, cardiovascular diseases and (acute and chronic) systemic diseases, are related to small variations in the concentration of various proteins in body fluids (Joo et al., 2012; Rathnayake et al., 2013; Wei et al., 2009). Therefore, the early detection of disease-marker proteins using highly sensitive methods can save lives and minimize time-consuming and inexpensive treatments. Biomarker detection is commonly conducted by laboratory methods suffering from high costs and long analysis times. Consequently, there is increasingly clinical demand to develop novel inexpensive biosensors or point-of-care (POC) devices that can provide more convenient test solutions (Cummins et al., 2016).

Among the body fluids tested in biosensors, saliva holds great promises in POC analysis (Nie et al., 2013; Tlili et al., 2010), mainly due to the economic and non-invasive manner of sampling. The salivary fluid can be easily and painlessly collected by either patients or health care personnel and requires no use of needles, thus reducing the probability of blood-borne infections and enhancing patient compliance. Owing to the presence of various salivary biomarkers accurately reflecting the disease condition in humans, salivary diagnostics has shown clinical relevance in monitoring a wide range of diseases and health complications. For example, saliva carries a series of interleukins (e.g. IL-1β and IL-8) and matrix metalloproteinases (e.g. MMP-8 and MMP-9) that can serve as biomarkers in a variety of human diseases including cancer, arthritis, cardiovascular disease and inflammatory disease (Rathnayake et al., 2013; Torrente-Rodríguez et al., 2015; Yang et al., 2005).

Accepted manuscript

ACCEPTED MANUSCRIPT

Optical immunosensors are a powerful detection and analysis tool for protein biomarkers in clinical diagnostics. For POC testing, the optical immunoassays are performed in either lateral-flow devices or microfluidic biosensors, benefiting from reduced sample and reagent consumption, rapid kinetics of antigen-antibody reaction at the surface and potential for automated fluid delivery into various reaction sites (Pires et al., 2013; Dong and Zhao, 2015; Yu et al., 2015). Among the optical detection methods, absorbance still remains an attractive choice in lateral flow and microfluidic biosensors due to its simplicity and easy readout. However, the small optical path length in microchannels affects the sensitivity of absorbance assays in microfluidic devices, as indicated by the Beer-Lambert law. The immunogold-silver assay (IGSA), involving silver ion reduction catalyzed by gold-colloid conjugated antibody, leads to the formation of a light-absorbing silver film that can be attached to the surface of the microfluidic chip (Sia et al., 2004). The attachment of the absorbing film may overcome the limitation of a small path length for detection, and the silver film is a simple and robust procedure for signal amplification in optical biosensors (Liu et al., 2011).

Despite the progresses in optical immunoassays, their successful implementation in practical POC devices still necessitates inexpensive optoelectronic technology (Chin et al., 2012). Conventional spectrophotometers and digital cameras are common in optical detection in microfluidic devices. These systems work as off-chip photodetectors due to their large dimensions, and are externally mounted to the microfluidic chips, which offers limited compactness to the biosensor. In alternative, silicon or inorganic photodiodes have been integrated to microfluidic devices (Jóskowiak et al., 2012; Pires et al., 2014; Zhang and Dong, 2013). These silicon devices enable flow-through assays to be performed in close proximity to the surface of the photodetector, and minute changes in light attenuation can be detected with

Accepted manuscript

ACCEPTED MANUSCRIPT

high sensitivity. Despite the advantages of silicon-based photodetectors, their expensive fabrication adds high cost to the POC device and hinders their use in a disposable biosensor. For example, the hydrogenated amorphous silicon photodiodes require plasma enhanced chemical vapor deposition, sputtering and a series of photolithography and etching processes (Jóskowiak et al., 2012). This fabrication procedure is in contrast to simple low-cost preparation of organic photodetectors (OPDs) by spin-coating, inkjet printing or spray-coating techniques (Wojciechowski et al., 2009).

Low temperature deposition of thin films in OPD fabrication opens the possibility of developing photodetectors monolithically integrated to typical polymer microfluidic chips. The size and shape versatility of the OPDs enables the photoactive area to match to the microchannel area where the optical assay is developed. This enhances system miniaturization while retaining highly sensitive optical detection with easy optical alignment (Charwat et al., 2013). Further, the band selectivity of OPDs are easily tunable by simple choice of organic molecule or polymer. The organic species can be either electron donors or acceptors in the photoactive layer, and are commonly mixed together to form unique architectures called bulk heterojunctions (BHJs). BHJs of poly(3-hexylthiophene) (P3HT) and (6,6)-phenyl-C_{61}-butyric-acid methyl-ester ($PC_{60}BM$), and BHJs of poly[N-9′-heptadecanyl-2,7-carbazole-alt-5,5-(4′,7′-di-2-thienyl-2′,1′,3′-benzothiadiazole)] (PCDTBT) and $PC_{70}BM$ have already been reported in microfluidic biosensors (Pires and Dong, 2014; Williams et al., 2014). Although these BHJ OPDs show high photosensitivity to wavelengths between 400-600 nm, they exhibit poor or no spectral response at 600-700 nm, which are wavelengths typically encountered in absorbance detection. Recent advances in organic solar cells have revealed the potential of BHJs of polythiophene derivatives and C_{70}-fullerene to exhibit remarkably high spectral responses at 600-700 nm (Yang et al.,

Accepted manuscript

ACCEPTED MANUSCRIPT

2015). In particular, BHJs of polythieno[3,4-b]thiophene/benzodithiophene (PTB7):$PC_{70}BM$ and poly[4,8-bis-substituted-benzo[1,2-b:4,5-b`]dithiophene-2,6-diyl-alt-4-substituted-thieno[3,4-b]thio-phene-2,6-diyl] (PBDTTT) derivatives:$PC_{70}BM$ hold promises to achieve quantum efficiencies approaching 70% at those wavelengths (Chen et al., 2009; Lu et al., 2014). Despite these enhanced characteristics, neither PTB7:$PC_{70}BM$ OPD nor PBDTTT-derivatives:$PC_{70}BM$ OPD has yet been exploited as photodetector in optical microfluidic biosensors.

Besides the BHJ photoactive layer, the standard device geometry of an OPD comprises an indium tin oxide (ITO) anode, an anode interfacial layer, normally poly(ethylenedioxythiophene): polystyrene sulphonate (PEDOT:PSS), and a Al cathode. Nevertheless, the structure of OPDs can be further improved by use of Ca as a cathode interfacial layer, which can reduce defects at the interface between the BHJ and Al. However, the use of Ca typically leads to poor device stability, due to its low work function, and its deposition is not compatible to spin coating or other solution-processable techniques (Wu et al., 2016). Efforts have thus been made to find spin-coated organic materials to replace Ca as cathode interfacial layers, thereby to achieve OPDs with outstanding performance while enhancing their low cost (Qi et al., 2015).

A novel optical microfluidic biosensor with polythiophene:$PC_{70}BM$ BHJ OPDs was developed in this work. The OPDs have comprised a solution-processable cathode interlayer, made of linear polyethylenimine (L-PEI), a polyethylenimine derivative. The photodetectors were integrated to a poly(methyl methacrylate) (PMMA) microfluidic chip, and measured light (~650 nm) absorbed by IGSA immunoassays conducted in the immuno-reaction chambers of the microfluidic chip (see Fig. 1). The salivary biomarkers in this study were detected to low picomolar concentration, comparable to the detection of same analyte by other reported

Accepted manuscript

ACCEPTED MANUSCRIPT

biosensors such as electrochemical magnetobiosensor (Torrente-Rodríguez et al., 2015) or fluorescence immunosensor (Tan et al., 2008). Furthermore, the novel device showed comparable accuracy to gold standard ELISA in measuring different concentrations of salivary biomarker in human saliva samples.

2 Materials and methods

2.1 Microfluidic chip and bio-functionalization

The PMMA microfluidic chip with high feature resolution was obtained by applying a milling process using a computerized numerical control machine (type CNC-JK40). Milling was applied to one 1-mm-thick PMMA plate to define openings for microchannels (0.2-mm height; 0.3-mm width; 4.5-mm long), chambers (~10-mm^3 volume), inlet (3-mm diameter) and outlets (1-mm diameter). The structured PMMA plate was thermally bonded with a bare PMMA slide (1-mm thickness) using a vacuum thermocompressor. The two slides were kept into contact under vacuum pressure of 0.57 MPa for 45 min at 80°C before bonded PMMA chip was obtained. The design of the microfluidic chip implied that the sample is loaded into the chip through only one inlet. The fluid is then guided along eight parallel microchannels and enters eight immuno-reaction chambers. The dimensions of the microchannels, chambers, inlet and outlets were optimized according to the fluid flow arrangement using a finite-element method (COMSOL Multiphysics™) (Honrado and Dong, 2014).

Following fabrication, the PMMA chip was functionalized with probe antibody specific to salivary biomarker. The bio-functionalization procedure is illustrated in Fig. S1 in Supporting information (SI). Briefly, the surface of the immuno-reaction chambers were first subjected to silanization after the fabricated chip was rinsed with ethanol and pre-treated with oxygen plasma.

Accepted manuscript

ACCEPTED MANUSCRIPT

An aminosilane, 3-aminopropyltriethoxysilane (APTES), was selected as the silanization agent, and a solution of APTES (Sigma-Aldrich, St. Louis, MO, USA) prepared in ~1% v/v in ethanol was incubated in the chip for 10 min at room temperature. This procedure was followed by rising the chip with toluene and ethanol so as to remove unbounded silane. Subsequently, the silanized PMMA surface was passivated using a biotin-containing PEG as the passivation layer. A solution of 1 mg mL^{-1} biotin-PEG-succinimidyl valerate and 6 mg mL^{-1} methoxy-PEG-succinimidyl valerate (both MW 5000, from Shanghai Yuduo Biological Technology Co., Ltd., China) was prepared in 100 mM bicarbonate buffer at pH 8 (Ploetz et al., 2014), and was incubated in the chip for over 8 h at room temperature. Further, to wash out unbound PEG/PEG-biotin, the chip was rinsed with distilled water and blow dried. The pegylated surface was thus ready for subsequent antibody immobilization. The biotin terminals of PEG/PEG-biotin layer was allowed to interact with 0.2 mg mL^{-1} NeutrAvidin (Sigma Aldrich) for 10 min at room temperature. Excess NeutrAvidin was removed from the chip by washing with phosphate-buffered saline (PBS). Bounded NeutrAvidin allowed covalent attachment of biotinylated probe antibody onto the PMMA chip. Prior to incubation, the probe antibody was diluted to a working concentration of ~10-20 nM in PBS and bovine serum albumin (BSA). After 10-min incubation the chip was rinsed with PBS-BSA. For sealing and further testing, a sterile and pierceable polyester cover foil (25 μm thick, ThinSeal™, EXCEL Scientific, Inc., Victorville, CA, USA) was added on top of the PMMA chip.

2.2 Polythiophene-C_{70} photodetector with L-PEI cathode interlayer

The OPDs of the optical microfluidic biosensor comprised the diode architecture of ITO/PEDOT: PSS/Polythiophene:$PC_{70}BM$/L-PEI/Al. The layout of the integrated OPD pixel is depicted in Fig. 1(a). The OPD devices were prepared onto patterned ITO coated on glass

Accepted manuscript

ACCEPTED MANUSCRIPT

substrates (thickness of ITO, 100 nm). For the active layer, PBDTTT-CF or PTB7 (Sigma Aldrich, both used as received) and $PC_{70}BM$ (Sigma Aldrich, used as received) were co-dissolved in a solvent mixture of 1,8-diiodoctane (3% v/v) in o-dichlorobenzene. The overall polymer weight ratio was 1:1.5 (10 mg mL^{-1}:15 mg mL^{-1}) and all solutions were stirred under a nitrogen atmosphere before use. The as-prepared solutions were spin-coated on the substrates, after the ITO/glass was pre-coated with PEDOT:PSS (Sigma Aldrich). The fabrication of the PBDTTT-CF:$PC_{70}BM$, PTB7:$PC_{70}BM$ and PEDOT:PSS layer was in a nitrogen-filled glove box, and the ITO/glass substrates were pre-treated with oxygen plasma at 50 W for 6 min prior to polymer deposition. A commercial profilometer was used to measure the polymer layer thicknesses. Further, following pre-treatment of the active layer, L-PEI was deposited onto the polythiophene:$PC_{70}BM$ BHJ via spin coating from methanol at 0.01wt% concentration (Wu et al., 2016). The resultant layer was baked at 90°C for 15 min. Finally, 100-nm-thick Al cathode was added onto L-PEI by thermal evaporation under vacuum pressure. The fabricated OPDs (0.1 cm^2 photoactive area) were encapsulated using UV-curable epoxy. The optoelectronic performance of the polythiophene:$PC_{70}BM$ OPD was characterized in terms of current density response and external quantum efficiency (EQE). EQE was determined as shown in SI.

Accepted manuscript

2.3 Immunogold-silver assay and testing procedure

The PMMA microfluidic chip with surface bio-functionalization was tested with IL-8, IL-1β, and MMP-8 in saliva. Artificial saliva samples at pH 7.2 were prepared by dissolving 0.6 mg mL^{-1} Na_2HPO_4, 0.6 mg mL^{-1} anhydrous $CaCl_2$, 0.4 mg mL^{-1} KCl, 0.4 mg mL^{-1} NaCl, 4 mg mL^{-1} mucin and 4 mg mL^{-1} urea in distilled water (Tlili et al., 2010). The salivary biomarkers were

ACCEPTED MANUSCRIPT

spiked in the artificial saliva solutions, and BSA was added to the spiked solutions to reduce probability of unspecific binding and aggregation. Human saliva samples were collected from adult subjects after informed consent was obtained. The biosensor tests with human saliva were conducted under consent from the subjects and in compliance with the relevance laws and ethical guidelines. All saliva samples were diluted 10× in distilled water prior to the tests with the integrated biosensor. Ten μL of diluted saliva sample was loaded into the microfluidic chip through the inlet, and vacuum was applied to the outlet until the entire sample filled up the immuno-reaction chamber. The incubation time for the sample containing the target salivary biomarker was 10 min.

The assay was completed by adding the gold-conjugated detection antibody and silver enhancer. Anti-IL-8 gold-labelled antibody in PBS-BSA solution was purchased from Wuhan Booute Biotechnology Co., Ltd. (China) and diluted before use. Polyclonal detection antibody against IL-1β and MMP-8 in PBS-BSA were obtained from Invitrogen Trading (Shanghai) Co., Ltd. and labelled with gold nanoparticles using the abcam® GOLD Conjugation Kit. Working solutions of <1 μg mL^{-1} detection antibody were loaded into the immuno-reaction chamber and allowed to incubate for 10 min. The unbound content was washed out from the chip using PBS and distilled water. The gold labels were then interacted with the silver enhancer. The solutions of silver salt and initiator, obtained from Sigma-Aldrich Silver Enhancer Kit, were mixed in equal volume ratio, and 10 μL of the resultant mixture was added into the microfluidic chip through the inlet. After an incubation period of 10 min at 20°C approximately, the autocatalytic reaction between gold conjugates and silver enhancer was stopped by removing the silver enhancer solution from the chip. This was followed by rinsing the immuno-reaction chambers with 2.5% sodium thiosulfate and distilled water.

Accepted manuscript

ACCEPTED MANUSCRIPT

After the IGSA assay procedures were conducted, the microfluidic chip was rapidly aligned between a commercial red LED (emitting ~650 nm) and the glass slide containing the polythiophene:$PC_{70}BM$ OPDs. A black-transparency sheet, with eight pinholes aligned with the OPDs, was placed on the glass slide with the surface contacting the bottom side of the PMMA chip. This black transparency served to prevent stray light reaching the OPDs. The immuno-reaction chambers in the microfluidic chip were placed over the pinholes, and their position was finely adjusted so as to maximize the matching area between the chambers and corresponding OPDs. The photocurrent, generated from the absorption of 650-nm photons by the OPDs, was measured using a Keithley 2600-type source measure unit. Recorded data was transferred to a PC via a USB-GPIB interface adapter. A second source measure unit was employed for the parallel multiplex measurements.

3 Results and discussion

3.1 Photodetector characterization and optimization

The photocurrent responses of the individual PBDTTT-CF:$PC_{70}BM$ OPD and PTB7:$PC_{70}BM$ OPD, modified with L-PEI, were characterized under visible-light conditions. For comparison, devices with cathodes made of only Al and OPDs with Ca/Al cathodes were also fabricated and tested. The results of short-circuit current density, J_{sc}, measured under 100 mW/cm^2 irradiation from a xenon lamp with an AM1.5 global filter, are shown in Fig. S2 in SI. The photocurrent of OPDs containing L-PEI did not differ significantly from those containing Ca. The L-PEI OPD has exhibited higher spectral response comparing to a device with Al solely. This is suggested by the EQE results displayed in Fig. 2(a). The differences in EQE between PBDTTT-CF:$PC_{70}BM$ devices containing L-PEI/Al and Al were 5% to 13% over the 500-700 nm spectrum. Moreover,

Accepted manuscript

EQE differences over 10% were also achieved by applying the L-PEI/Al cathode to the PTB7:$PC_{70}BM$ OPD. The enhanced EQE with the L-PEI/Al cathode correlated to higher J_{sc}, as seen in Fig. S2, and indicated that with L-PEI more incident photons were converted into measurable charge carriers. This improvement has derived from the formation of dipoles at the interface between the polythiophene:$PC_{70}BM$ layer and cathode, as further described in SI.

EQE was further determined for various nano-thicknesses of PBDTTT-CF:$PC_{70}BM$ in L-PEI OPDs under illumination of 650-nm monochromatic light. An EQE of ~70% was obtained for an active layer thickness of 95 nm, as observed in Fig. 2(b). This result may have reflected the good compromise between charge transport and photon absorption. Thicker active layers would lead to enhanced photon absorption; however, the decreased EQE responses for PBDTTT-CF:$PC_{70}BM$ thicknesses between 105 and 140 nm may have mainly attributed to the reduced charge transport efficiency in those thicker layers.

The photodetector with 95-nm-thick PBDTTT-CF:$PC_{70}BM$ was then used to detect streptavidin-gold nanoparticles (10 nm) conjugate in the PMMA chip. The streptavidin-gold conjugate (Cytodiagnostics, Ontario, Canada) was diluted into several concentrations prepared in PBS/BSA. The resultant solutions were applied to the surface of the PMMA chip passivated with PEG/PEG-biotin, followed by incubation with the silver enhancer solution. These tests served to demonstrate the effectiveness of PEG-biotin passivation before antibody was applied to the surface of the chip. The results plotted in Fig. S3 have demonstrated a decrease in photocurrent by applying increasing concentrations of streptavidin-gold. The good consistency of these results indicated the presence of biotin onto the surface of the chip. Streptavidin has strongly interacted with biotin, and as more streptavidin were added into the chip, as more opaque became the

Accepted manuscript

ACCEPTED MANUSCRIPT

reduced silver film. The enhanced opacity due to increasing streptavidin-gold concentrations was confirmed by absorbance measurements with a bench-top UV/Vis absorbance plate.

Further tests with streptavidin-gold have been conducted to optimize the PEDOT:PSS layer in the L-PEI modified PBDTTT-CF:$PC_{70}BM$ OPD. Devices with PEDOT:PSS nano-thicknesses varying between 25 nm and 80 nm were fabricated, and three streptavidin-gold concentrations were detected in the PMMA chip. Higher J_{sc} was achieved for a PEDOT:PSS thickness of 40 nm for all analyte concentrations, and the decreased thicknesses from 80 to 40 nm have led to an improvement of the detector response, as observed in Fig. 2(c). This may have resulted from the enhancement of charge carrier (holes) transfer and extraction through the ITO anode of the devices, as illustrated in Fig. 1(a). The 40-nm-thick PEDOT:PSS has also led to lower baseline photocurrent, J_d, as measured by switching off the red LED and conducted before the streptavidin-gold conjugate and silver enhancer solution were added into the chip. The minimum J_d, as observed in Fig. 2(d), indicates an improvement in the noise (dark current) characteristics of the OPD. Overall, the higher J_{sc} and lower J_d obtained with the 40-nm-thick PEDOT:PSS in the presence of L-PEI can lead to OPDs exhibiting a remarkably high signal-to-noise ratio.

Accepted manuscript

3.2 Immunodetection with optical microfluidic biosensor

After the PBDTTT-CF:$PC_{70}BM$ photodetector was optimized, the optical microfluidic biosensor was tested with saliva samples spiked with IL-8, IL-β and MMP-8. Figure 3(a) plots the photocurrent response due to detection of IL-8, IL-1β and MMP-8 concentrations by IGSA assays conducted in separate PMMA microfluidic chips. The immuno-chambers of these chips were previously functionalized with probe antibodies specific to the corresponding biomarkers.

ACCEPTED MANUSCRIPT

The photocurrent data were fitted to sigmoidal curves (Boltzmann) with a correlation coefficient of 0.995 for IL-8, 0.991 for IL-1β and 0.993 for MMP-8. Relative standard deviation (RSD) values did not exceed 10.3%, 8.6% and 10.6% for IL-8, IL-1β and MMP-8, respectively, according to multiple independent measurements of same concentration of biomarker. Further, the limits of detection (LODs) were calculated to be 90 pg mL^{-1} (1.07 pM) for IL-8, 80 pg mL^{-1} (4.57 pM) for IL-1β and 120 pg mL^{-1} (2.35 pM) for MMP-8, as from the results of 3× standard deviation of five blank tests.

The LOD achieved for salivary IL-8 did not differ significantly from that obtained with an electrochemical magnetobiosensor and a fluorescence immunosensor (see Table 1). The LOD result was also comparable to that of an ELISA spectrophotometric assay that required an industrial plate reader for photo-detection. The bulky plate readers are hardly used in situ due to their high costs and need for specialized operators, and hence not recommended for routine checking of bio-fluids in POC settings. The PBDTTT-CF:$PC_{70}BM$ OPD hold great promises as a portable and cost-effective device, which coupled with a simple immunoassay as IGSA makes it a very attractive and user-friendly tool to realize POC analysis. Moreover, the IL-8 LOD result was remarkably lower in two orders of magnitude than that of a SPR immunosensor coupled with another bulky signal reader. It is also worth to remark that the IL-8 LOD was over six-fold lower than the clinical cut-off value of 600 pg mL^{-1} in saliva, which was established to differentiate oral cancer patients from healthy individuals (John et al., 2004).

Comparing to other optical biosensors employing the IGSA immunoassay, the obtained LODs did not differ significantly from 30 pg mL^{-1} achieved by Liu et al. (2011) and 15 pg mL^{-1} achieved by Kim et al. (2015). These previously reported IGSA immunosensors were performed in non-microfluidic environments and used bulky plate readers for the absorbance measurements.

Accepted manuscript

ACCEPTED MANUSCRIPT

To obviate the use of regular laboratory equipment for assay readings, Sia et al. (2004) and Ahn et al. (2010) have employed compact and miniaturized photodetectors to IGSA assays conducted in microchips. Sia et al. (2004) have obtained an LOD of 89 pM using an integrated inorganic photodiode, while Ahn et al. (2010) estimated an LOD of 1 ng mL^{-1} employing an amorphous silicon photodetector. Moreover, the polythiophene:$PC_{70}BM$ organic photodetector differs from the inorganic analogs by the possibility of developing disposable biosensors due to simpler and less expensive fabrication procedure.

In regard to assay analysis time, the optical microfluidic biosensor can perform the test in 30 min, including incubation times for the sample, gold-labelled antibody and silver enhancer solution. This analysis time was similar to that of the IGSA assays mentioned above, and was shorter than that of the aforementioned electrochemical magnetobiosensor and fluorescence immunosensor (see Table 1). Further, commercial Luminex® xMAP assays and ELISA methods coupled with bulky optical detection instrumentation typically take over two hours to obtain the analytical result for salivary protein biomarkers.

The specificity of detection was analyzed by conducting all IL-8, IL-1β and MMP-8 assays in four immuno-chambers of the biosensor. Three chambers were coated with probe antibody specific to IL-8, IL-1β and MMP-8, respectively, while the fourth chamber was left blank. Three saliva samples were prepared with 500 pg mL^{-1} IL-8, 500 pg mL^{-1} IL-1β, 1000 pg mL^{-1} MMP-8 for the assays. No significant photocurrent variation was encountered in IL-8, IL-1β and MMP-8 assays performed in non-corresponded chambers, comparing to the results from the blank chamber [see Fig. 3(b)]. The RSD values for IL-8, IL-1β and MMP-8 in non-corresponded chambers did not exceed 3.1%. The slight decrease in ΔS might have been caused by poor washing of the PMMA chip between assays. The presence of PEG in the passivated chip has

Accepted manuscript

ACCEPTED MANUSCRIPT

prevented larger ΔS decreasing via unspecific protein adsorption. The slightly decreased ΔS values from the non-specificity tests was importantly not lower than the LODs of the targeted salivary biomarkers.

3.3 Multiplexed salivary biomarker detection

Multiplex assays were performed with the biosensor. As indicated by the layout shown in Fig. 1, the device can detect up to eight analytes in parallel. In this study, IL-8, IL-1β and MMP-8 were detected in the saliva sample at one time. Figure 4 shows the detection results from four multiplex saliva samples #1 to #4. The ΔS values from four concentrations of IL-8, IL-1β and MMP-8 as obtained from the corresponding calibration curves were also plotted. The concentrations of IL-8, IL-1β and MMP-8 in the multiplex samples were all discriminated by the biosensor. As an example, the ΔS values for 200 pg mL^{-1} IL-8 present in samples #1 and #2 were between those of 125 pg mL^{-1} and 300 pg mL^{-1} [see Fig. 4(a)]. As shown in Fig. 4(b), the results for 125 pg mL^{-1} IL-1β in samples #1 and #3 lie between 100 pg mL^{-1} and 150 pg mL^{-1}. For MMP-8 in samples #2 and #4, the ΔS value corresponded to 600 pg mL^{-1} was measured between 500 pg mL^{-1} and 850 pg mL^{-1} [see Fig. 4(c)]. These tests have indicated that the optical microfluidic biosensor can accurately measure the concentration of multiple analytes from one sample.

Accepted manuscript

ACCEPTED MANUSCRIPT

3.4 Detection of human salivary IL-8 and IL-1β

The biosensor was further tested with human saliva samples. IL-8 and IL-1β was targeted and their salivary levels were measured using two ELISA absorbance detection kits (Human IL-8 ELISA and Human IL-1β ELISA, Invitrogen Trading Co., Ltd) and a standard plate reader. Two groups of IL-8 concentration, 250±31 pg mL^{-1} (n=7, low concentration group) and 750±40 pg mL^{-1} (n=7, high concentration group), and two groups of IL-1β, 94±13 pg mL^{-1} and 240±17 pg mL^{-1} (both n=7) were used to evaluate the optical microfluidic device. The estimated values of concentration from the device were obtained from the calibration curves. The test data shown in Fig. 5(a) and Fig. 5(b) indicated that the results obtained with the biosensor correlated well with the measurements performed with ELISA (R^2=0.96 for IL-8, R^2=0.97 for IL-1β). Although the estimated values were (< two-fold) higher than ELISA, the biosensor was able to discriminate the low concentration group from the high concentration group for both IL-8 and IL-1β (P<0.01, using the Wilcoxon signed-ranks test). The measurement differences encountered between the biosensor and ELISA may have caused by viscosity variation between the real saliva and artificial saliva (used as the standard solution for the calibration curves). The presence of remaining protein impurities (e.g. enzymes) in real saliva might have increased the estimated concentrations with the biosensor at some extent.

Accepted manuscript

ACCEPTED MANUSCRIPT

4 Conclusions

An optical microfluidic biosensor with polythiophene:$PC_{70}BM$ BHJ OPDs for the detection of clinically relevant salivary biomarkers is described in this work. The biosensor has demonstrated good analytical performance for salivary IL-8, IL-1β and MMP-8, exhibiting low detection limits, high detection specificity and reproducibility. The LOD for IL-8 was below the clinical established cut-off of 600 pg mL^{-1}, and was in same range as that of other previously reported immunosensors such as those utilizing electrochemical or fluorescence detection. The OPDs have incorporated a polymer cathode interlayer made of L-PEI compatible to solution-processable methods, which enhances the low cost of the organic photodetector and resultant biosensor.

The biosensor was further tested with human saliva samples, and the results were bench marked against two conventional absorbance assays of ELISA. Measurements of salivary biomarker concentrations were statistically correlated to those provided by ELISA. However, on contrary to ELISA performed with bulky optical instrumentation, the optical microfluidic biosensor can easily be realized in a portable and cost-effective device which makes it very attractive to POC settings. The proposed biosensor can also be extended to the detection of other protein biomarkers using other antibodies, thus finding application in diagnostics and screening of multiple diseases.

Acknowledgments

This work was supported by the National Natural Science Foundation of China (grant no. 61550110253 and 61650410655), and by Regionale forskningsfond Oslofjordfondet (proj. no.

Accepted manuscript

ACCEPTED MANUSCRIPT

234972, proj. no. 249017, proj. no. 258902 and proj. no. 260586). The authors thank Li Linbo for assistance and discussions on OPD fabrication processes. School of Mechanical Eng. in Nanjing University of Science & Technology and the Out-patient Dept. at Chongqing Xiji Hospital are acknowledged for supporting the experimental work.

References

Ahn, C.-G., Ah, C.S., Kim, T.Y., Park, C.W., Yang, J.-H., Kim, A., Sung, G.Y., 2010. Appl. Phys. Lett. 97, 103703.

Charwat, V., Purtscher, M., Tedde, S.F., Hayden, O., Ertl, P., 2013. Lab Chip 13, 785–797.

Chen, H.-Y., Hou, J., Zhang, S., Liang, Y., Yang, G., Yang, Y., Yu, L., Wu, Y., Li, G., 2009. Nat. Photonics 3, 649–653.

Chin, C.D., Linder, V., Sia, S.K., 2012. Lab Chip 12, 2118–2134.

Cummins, B.M., Ligler, F.S., Walker, G.M., 2016. Biotechnol. Adv. 34, 161–176.

Dong, T., Zhao, X., 2015. Anal. Chem. 87, 2410–2418.

Honrado, C., Dong, T., 2014. J. Micromech. Microeng. 24, 125023.

John, M.A.R.S., Li, Y., Zhou, X., Denny, P., Ho, C.-M., Montemagno, C., Shi, W., Qi, F., Wu, B., Sinha, U., Jordan, R., Wolinsky, L., Park, N.-H., Liu, H., Abemayor, E., Wong, D.T.W., 2004. Arch. Otolaryngol. Head Neck Surg. 130, 929–935.

Joo, J., Kwon, D., Yim, C., Jeon, S., 2012. ACS Nano 6, 375–4381.

Jóskowiak, A., Stasio, N., Chu, V., Prazeres, D.M.F, Conde, J.P., 2012. Biosens. Bioelectron. 36, 242–249.

Accepted manuscript

ACCEPTED MANUSCRIPT

Kim, W.-J., Cho, H.Y., Kim, B.K., Huh, C., Chung, K.H., Ahn, C.-G., Kim, Y.J., Kim, A., 2015. Sens. Act. B. Chem. 221, 537–543.

Liu, R., Liu, X., Tang, Y., Wu, L., Hou, X., Lv, Y., 2011. Anal. Chem. 83, 2330–2336.

Lu, L., Xu, T., Chen, W., Landry, E.S., Yu, L., 2014. Nat. Photonics 8, 716–722.

Nie, S., Benito-Peña, E., Zhang, H., Wu, Y., Walt, D.R., 2013. Anal. Chem. 85, 9272–9280.

Pires, N.M.M., Dong, T., 2014. J. Biomed. Opt. 19(3), 030504.

Pires, N.M.M., Dong, T., Hanke, U., Hoivik, N., 2013. J. Biomed. Opt. 18, 097001.

Pires, N.M.M., Dong, T., Hanke, U., Hoivik, N., 2014. Sensors 14, 15458–15479.

Ploetz, E., Visser, B., Slingenbergh, W., Evers, K., Martinez-Martinez, D., Pei, Y.T., Feringa, B.L.M., De Hosson, J.Th.M., Cordes, T., van Dorp, W.F., 2014. J. Mater. Chem. B 2, 2606–2615.

Qi, B., Zhang, Z.-G., Wang, J., 2015. Sci. Rep. 5, 7803.

Rathnayake, N., Åkerman, S., Klinge, B., Lundegren, N., Jansson, H., Tryselius, Y., Sorsa, T., Gustafsson, A., 2013. Plos One 8, e61356.

Sia, S.K., Linder, V., Parviz, B.A., Siegel, A., Whitesides, G.M., 2004. Angew. Chem. Int. Ed. 43, 498–502.

Tan, W., Sabet, L., Li, Y., Yu, T., Klokkevold, P.R., Wong, D.T., Ho, C.-M., 2008. Biosens. Bioelectron. 24, 266–271.

Tlili, C., Cella, L.N., Myung, V.N., Shetty, V., Mulchandani, A., 2010. Analyst 135, 2637–2642.

Torrente-Rodríguez. R.M., Campuzano, S., Montiel, V.R.-V., Gamella, M., Pingarrón, J.M., 2015. Biosens. Bioelectron. 77, 543–548.

Williams, G., Backhouse, C., Aziz, H., 2014. Electronics 3, 43–75.

Wei, F., Patel, P., Liao, W., Chaudhry, K., Zhang, L., Arellano-Garcia, M., Hu, S., Hu, S., Elashoff, D., Zhou, H., Shukla, S., Shah, F., Ho, C.M., Wong, D.T., 2009. Clin.Cancer Res. 15, 4446–4452.

Wojciechowski, J.R., Shriver-Lake, L.C., Yamaguchi, M.Y., Fureder, E., Pieler, R., Schamesberger, M., Winder, C., Prall, H.J., Sonnleitner, M., Ligler, F.S., 2009. Anal. Chem. 81, 3455–3461.

Wu, F.-C., Tung, K.-C., Chou, W.-Y., Tang, F.-C., Cheng, H.-L., 2016. Org. Electron. 29, 120–126.

Accepted manuscript

ACCEPTED MANUSCRIPT

Yang, C.-Y., Brooks, E., Li, Y., Denny, P., Ho, C.-M., Qi, F., Shi, W., Wolinsky, L., Wu, B., Wong, D.T.W., Montemagno, C.D., 2005. Lab Chip 5, 1017–1023.

Yang, Y., Chen, W., Dou, L., Chang, W.-H., Duan, H.-S., Bob, B., Li, G., Yang, Y., 2015. Nat. Photonics 9, 190–198.

Yu, Z.T.F., Guan, H., Cheung, M.K., McHugh, W.M., Cornell, T.T., Shanley, T.P., Kurabayashi, K., Fu, J., 2015. Sci. Rep. 5, 11339 (2015).

Zhang, L., Dong, T., 2013. J. Micromech. Microeng. 23, 045011.

Fig. 1 Layout of the optical microfluidic biosensor with L-PEI modified polythiophene-C_{70} OPDs. (a) Schematic overview of the biosensor including layout details for the OPD. Light at the wavelength absorbed by the IGSA immunoassay is measured as photocurrent by the OPD. AuNPs, gold nanoparticles. (b) Tridimensional scheme and photographs of device layers. The photoactive area of eight OPDs matches to surface area of eight immuno-reaction chambers of the PMMA microfluidic chip. Device layers are not to scale.

Fig. 2 Optoelectronic performance of the L-PEI modified polythiophene-C_{70} OPD. (a) EQE spectra of the PBDTTT-CF:$PC_{70}BM$ OPD with and without the L-PEI cathode interfacial layer. (b) EQE spectra measured at 650 nm for L-PEI OPDs with varying thicknesses of PBDTTT-CF:$PC_{70}BM$. (c) Current density response of the L-PEI modified PBDTTT-CF:$PC_{70}BM$ OPD as a function of PEDOT:PSS thickness. Three streptavidin-gold concentrations were detected for each PEDOT:PSS thickness. (d) Baseline current density measured in OPDs with varying PEDOT:PSS thicknesses. The measurements of baseline current were conducted in dark.

Accepted manuscript

ACCEPTED MANUSCRIPT

Fig. 3 Immuno-detection of salivary biomarkers by performing IGSA assays with the optical microfluidic biosensor. (a) Dose-response curves obtained from the detection of IL-8, IL-1β and MMP-8. ΔS was determined as the ratio of photocurrent due to each biomarker concentration to that measured with no presence of biomarker (0 pg mL^{-1}). (b) Tests of biosensor specificity by detecting each of IL-8, IL-1β and MMP-8 in four immuno-chambers. Three chambers were modified with specific antibody, and the remained one was left blank. Error bars in (a) and (b) represent standard deviation for triplicate tests (n=3).

Fig. 4 Immuno-detection of salivary biomarkers from multiplex saliva samples. (a) Detection of IL-8 from four saliva samples labelled as #1, #2, #3 and #4. The concentration of IL-8 was 200 pg mL^{-1} in #1 and #2 and 350 pg mL^{-1} in #3 and #4. (b) Detection of IL-β from saliva samples #1, #2 and #3. The concentration of IL-β in #1 and #3 was 125 pg mL^{-1}, and IL-1β concentration in #2 was 300 pg mL^{-1}. (c) Detection of MMP-8 from saliva samples #2, #3 and #4. MMP-8 concentration was 600 pg mL^{-1} in #2 and #4 and 1000 pg mL^{-1} in #3. The x axis displays biomarker concentration in pg mL^{-1}, and error bars are standard deviation for triplicate tests (n=3).

Fig. 5 Detection of human salivary IL-8 and IL-1β using the optical microfluidic biosensor. The plots (a) and (b) show the measured results of two groups of IL-8 concentration and two groups of IL-1β concentration, respectively, as detected by ELISA in parallel.

Table 1 LOD and analysis time for the detection of salivary IL-8 using the optical microfluidic biosensor and previously reported biosensors and standard methods.

Accepted manuscript

ACCEPTED MANUSCRIPT

LOD (pg mL^{-1})	Analysis time	Immunoassay	Detector	Reference
90	30 min	IGSA	OPD	This work
72.4	5h	Magneto-electrochemical	Screen-printed carbon electrode	Torrente-Rodríguez et al., 2015
92	75 min	Fluorescence	Digital camera	Tan et al., 2008
1650	15 min	Surface plasmon resonance	Bulky SPR reader	Yang et al., 2005
7.4	10 min	Electrochemical	Gold electrodes	Wei et al., 2009
25	17h	ELISA	Spectrophotometer	Torrente-Rodríguez et al., 2015
4	> 2h	Fiber-optic fluorescence	Digital camera	Nie et al., 2013
0.5	> 2h	Luminex xMAP	Bulky plate reader	Rathnayake et al., 2013

Accepted M

Highlights

- A novel optical microfluidic biosensor with integrated polythiophene-C_{70} OPDs.
- Compact, miniaturized device for detection of salivary biomarkers at point of care.
- OPDs with polyethylenimine-modified cathode for low-cost and sensitive biosensors.
- Detection limit of few pM for salivary IL-8, IL-1□ and MMP-8 was achieved.
- Absorbance detection of protein markers in human saliva with a microfluidic chip.

Figure 1

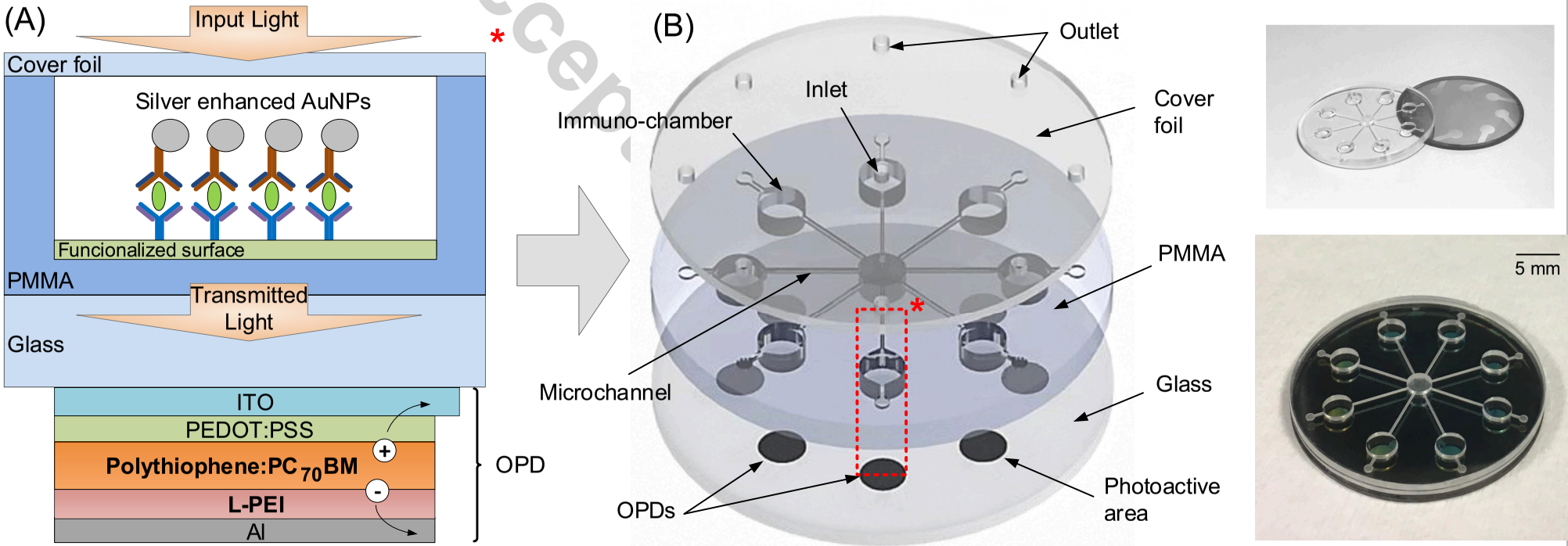

ACCEPTED MANUSCRIPT

Figure 2

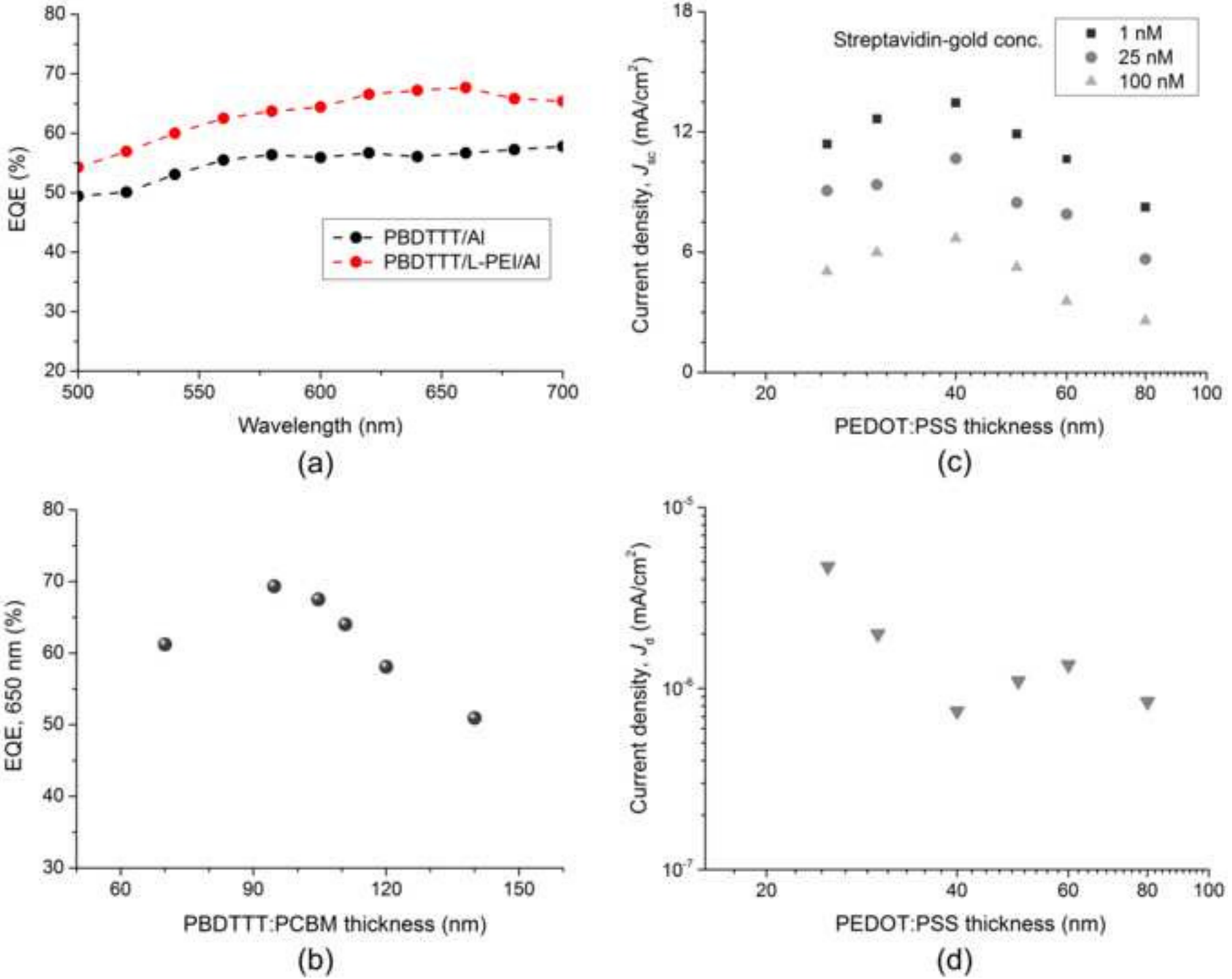

ACCEPTED MANUSCRIPT

Figure 3

ACCEPTED MANUSCRIPT

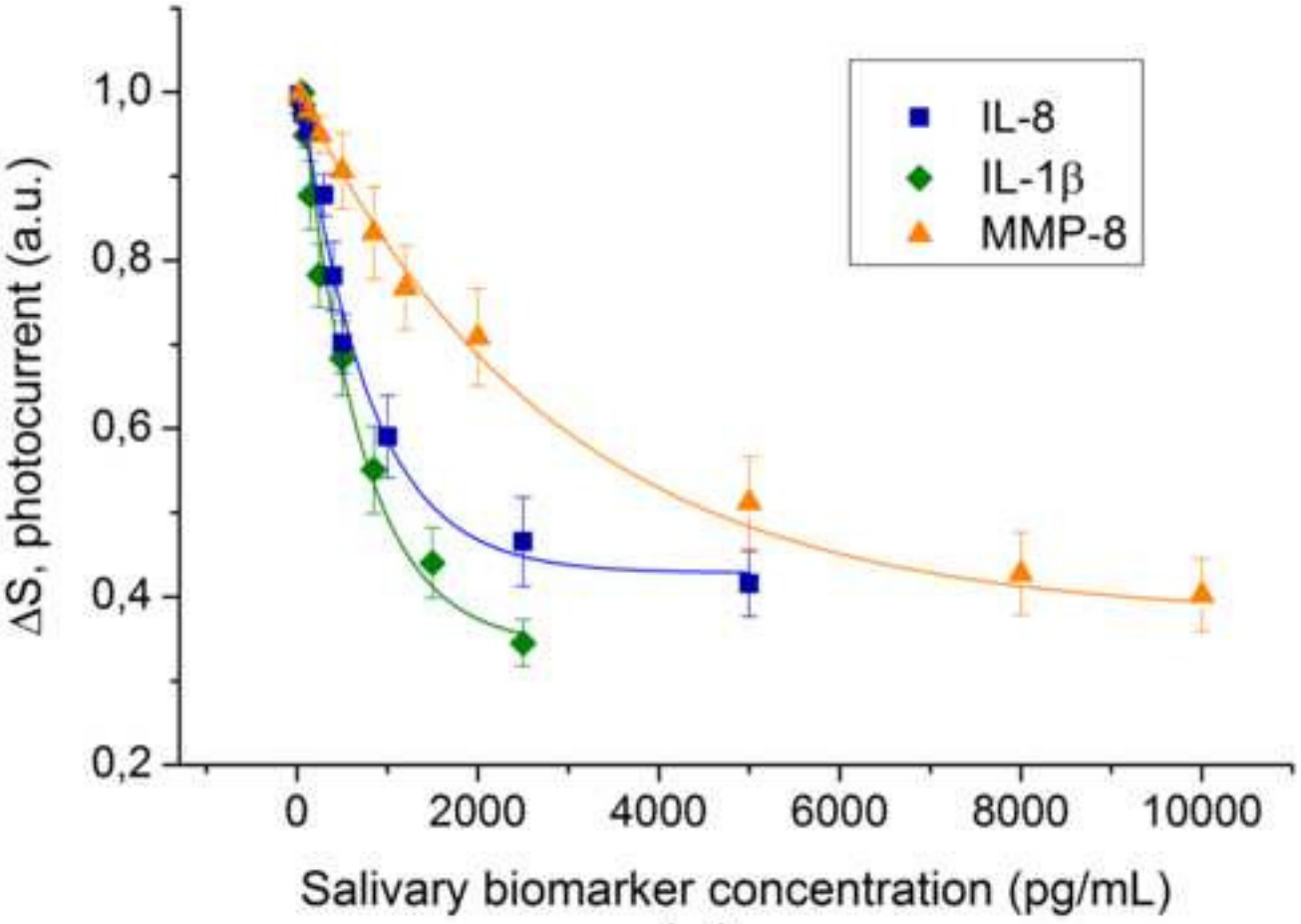

(a)

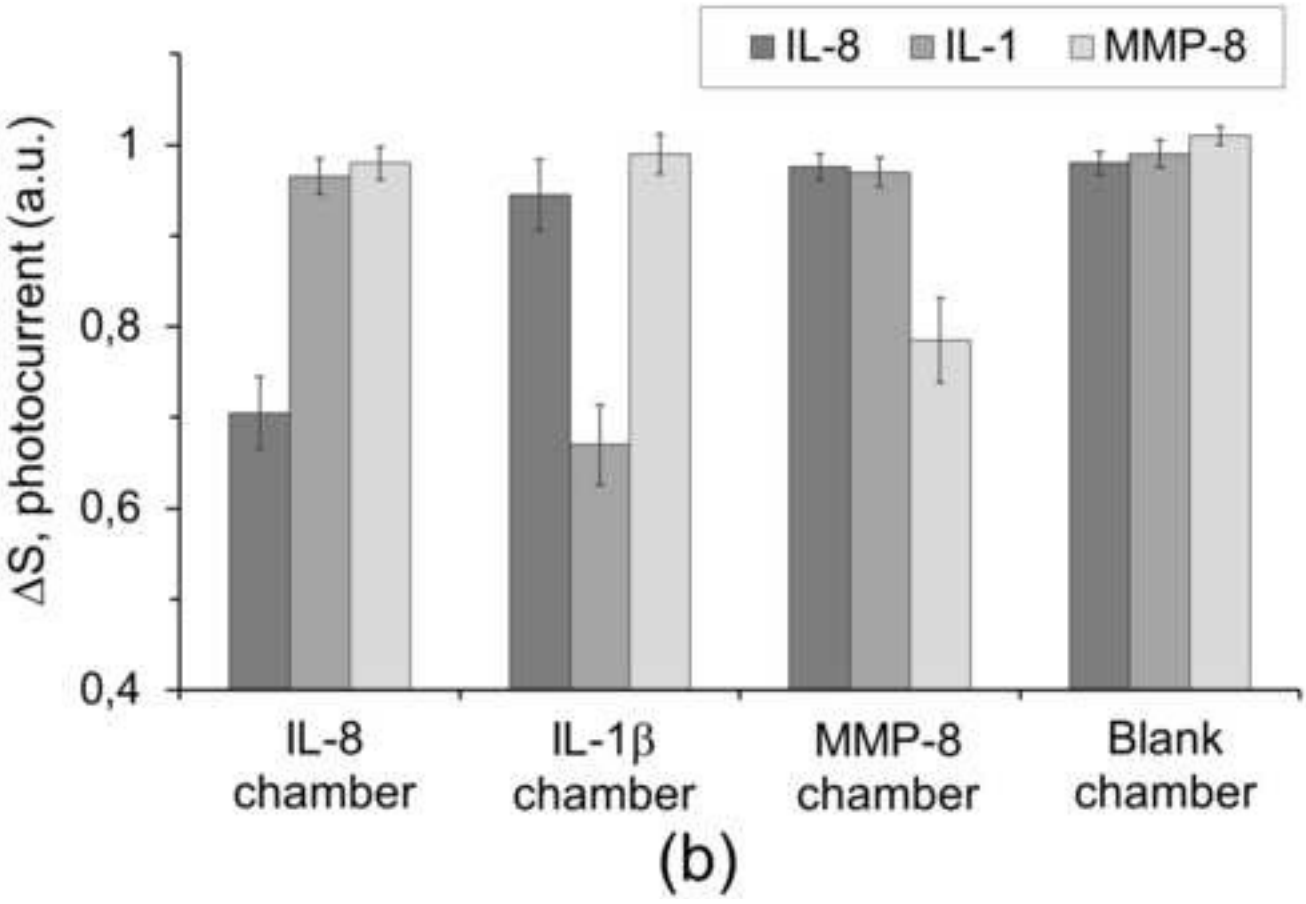

(b)

ACCEPTED MANUSCRIPT

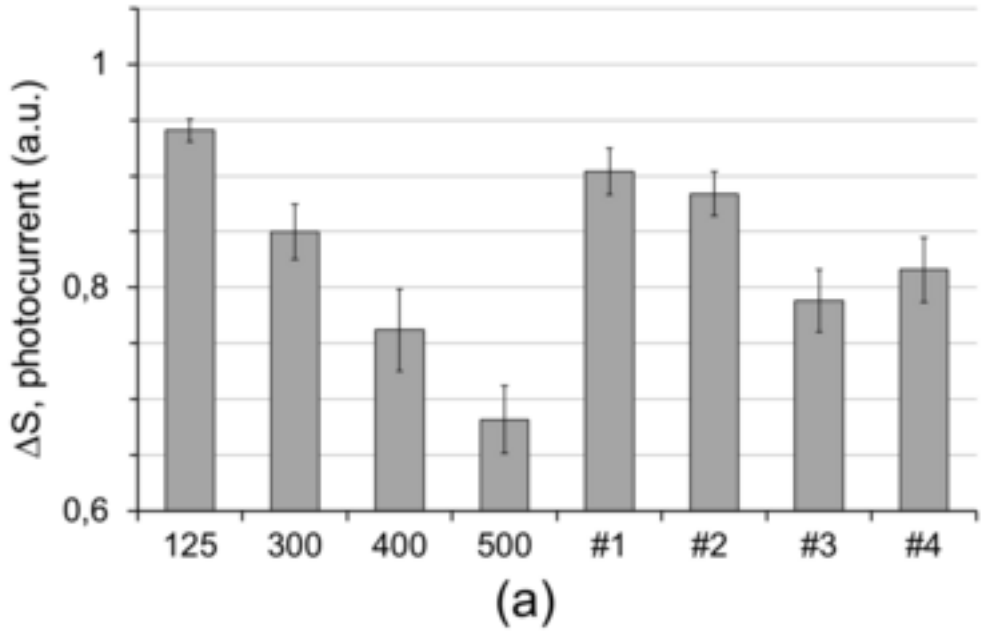

(a)

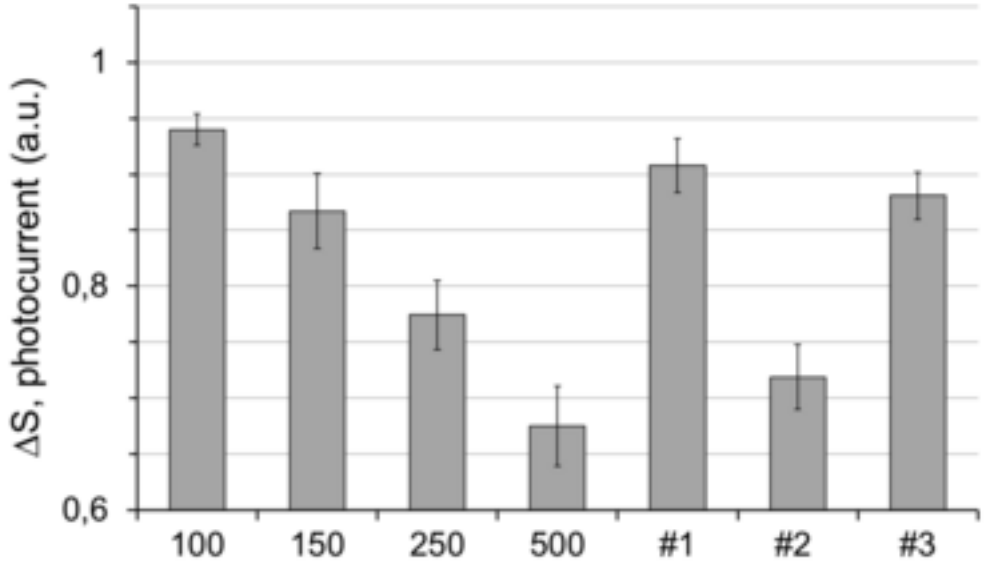

(b)

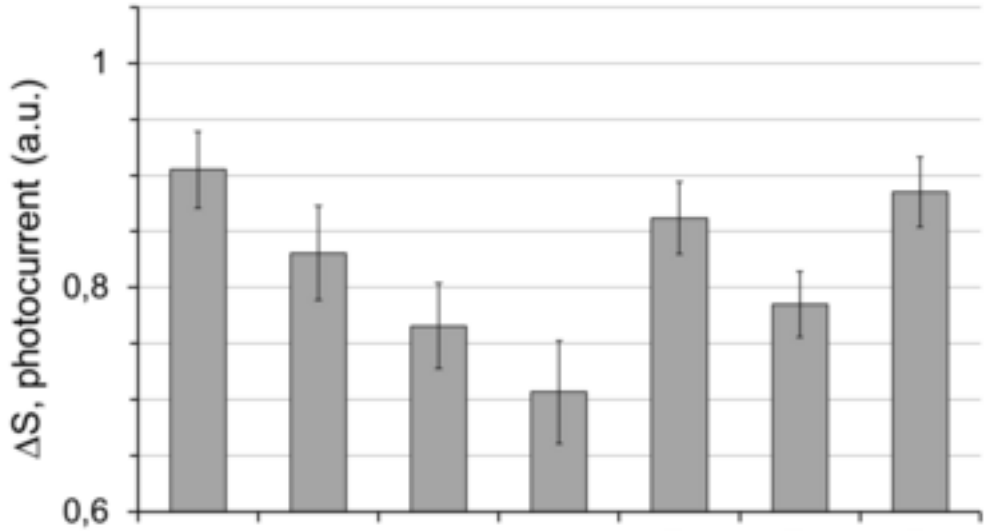

(c)

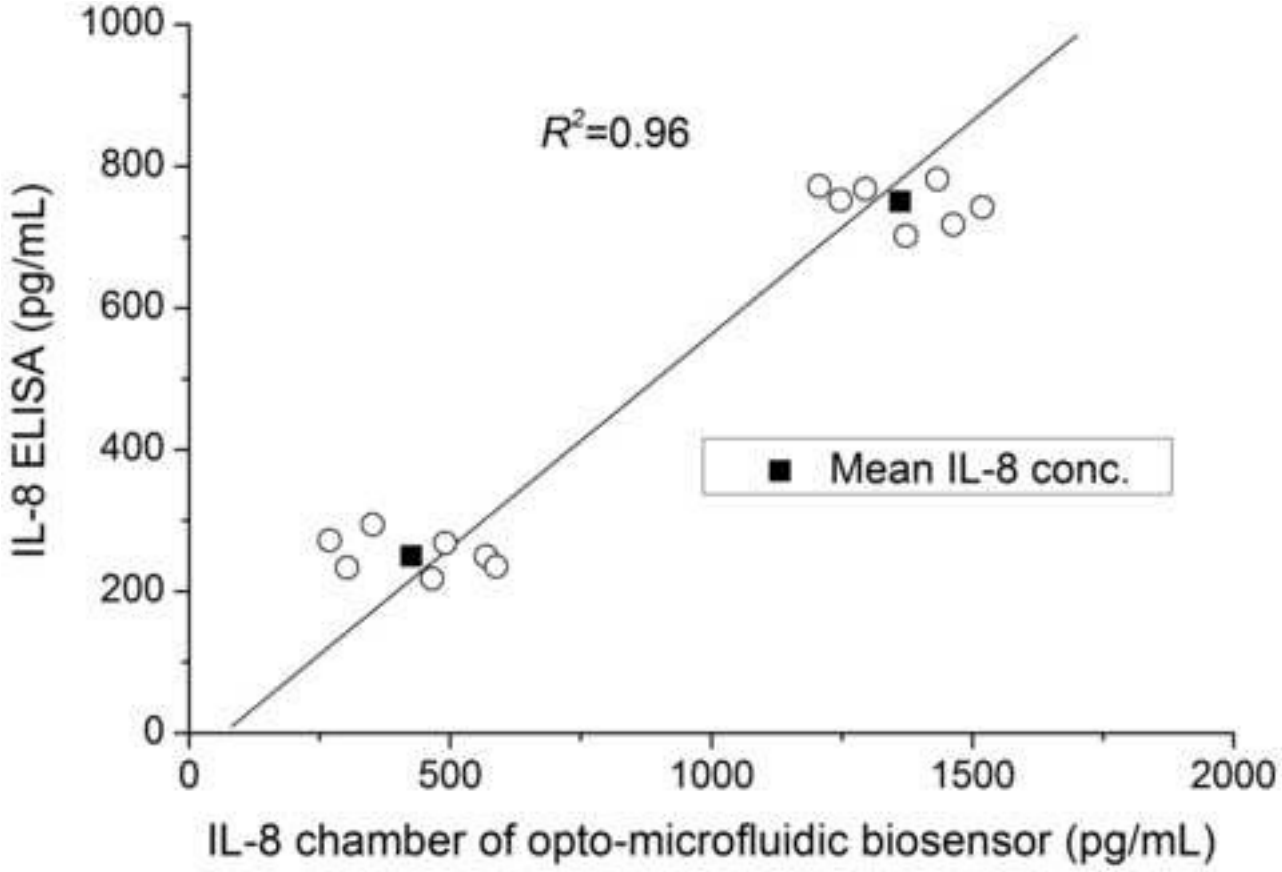
1000
800
600
400
200
0
IL-8 ELISA (pg/mL)
R^2=0.96
Mean IL-8 conc.
0
500
1000
1500
2000
IL-8 chamber of opto-microfluidic biosensor (pg/mL)

(a)

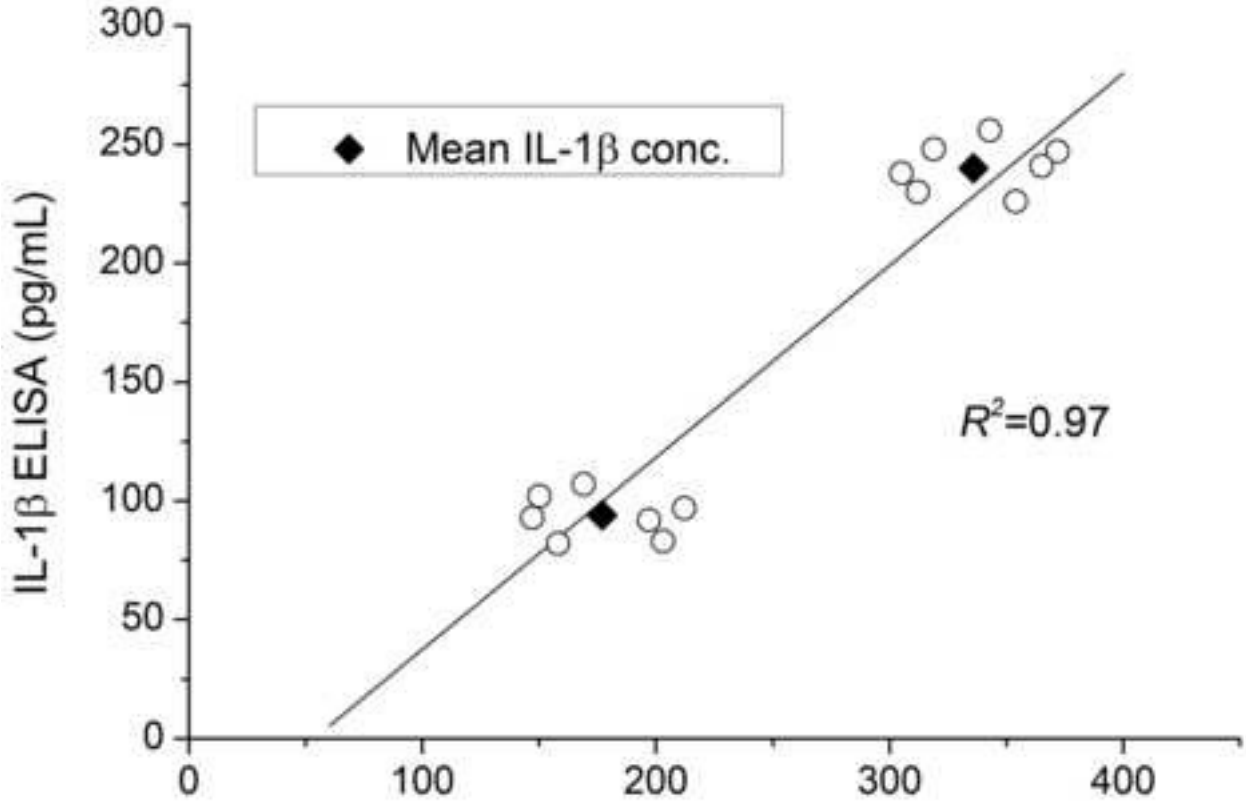
300
250
200
150
100
50
0
IL-1β ELISA (pg/mL)
Mean IL-1β conc.
R^2=0.97
0
100
200
300
400
IL-1β chamber of opto-microfluidic biosensor (pg/mL)

(b)